

Some Remarks on Methods of QCD Analysis of Polarized DIS Data

Elliot Leader

Imperial College London

Prince Consort Road, London SW7 2BW, England

Aleksander V. Sidorov

Bogoliubov Theoretical Laboratory

Joint Institute for Nuclear Research, 141980 Dubna, Russia

Dimiter B. Stamenov

CERN, Theory Division, CH 1211 Geneva 23, Switzerland,

Institute for Nuclear Research and Nuclear Energy

Bulgarian Academy of Sciences

Blvd. Tsarigradsko Chaussee 72, Sofia 1784, Bulgaria

Abstract

The results on polarized parton densities (PDFs) obtained using different methods of QCD analysis of the present polarized DIS data are discussed. Their dependence on the method used in the analysis, accounting or not for the kinematic and dynamic $1/Q^2$ corrections to spin structure function g_1 , is demonstrated. It is pointed out that the precise data in the preasymptotic region require a more careful matching of the QCD predictions to the data in this region in order to determine the polarized PDFs correctly.

1 Introduction

Our present knowledge of the spin structure of the nucleon comes mainly from polarized inclusive and semi-inclusive DIS experiments at SLAC, CERN, DESY and JLab, polarized proton-proton collisions at RHIC and polarized photoproduction experiments. One of the important and best studied aspects of this knowledge is the determination, in a QCD framework, of the longitudinal polarized parton densities and their first moments, which are related to the spins carried by the quarks and gluons in the nucleon. Different methods of analysis have been used in these studies. The aim of this paper is to discuss and clarify how the results on polarized PDFs depend on the method used in the QCD analysis.

One of the peculiarities of polarized DIS is that more than a half of the present data are at moderate Q^2 and W^2 ($Q^2 \sim 1 - 4 \text{ GeV}^2$, $4 \text{ GeV}^2 < W^2 < 10 \text{ GeV}^2$), or in the so-called *preasymptotic* region. So, in contrast to the unpolarized case, this region cannot be excluded from the analysis, and the role of the $1/Q^2$ terms (*kinematic* - γ^2 factor, target mass corrections, and *dynamic* - higher twist corrections to the spin structure function g_1) in the determination of the polarized PDFs has to be investigated. This makes the QCD analysis of the data much more complicated and difficult than in the unpolarized case.

2 QCD framework for inclusive polarized DIS

2.1 Which data to chose for QCD fits

The best manner to determine the polarized PDFs is to perform a QCD fit to the data on g_1/F_1 , which can be obtained if both the $A_{||}$ and A_{\perp} asymmetries are measured. In some cases only $A_{||}$ is measured. One can write (D is the depolarization factor and $\gamma^2 = 4M^2x^2/Q^2$)

$$\frac{A_{||}}{D} = A_1 + \eta A_2 = (1 + \gamma^2) \frac{g_1}{F_1} + (\eta - \gamma) A_2, \quad (1)$$

from which one sees that the quantity $A_{||}/D(1 + \gamma^2)$ is a good approximation of g_1/F_1 because the second term in the second relation of (1) can be neglected in the preasymptotic region too - the asymmetry A_2 is bounded and in fact small, and multiplied in addition by a small kinematic factor ($\eta \approx \gamma$).

The data on the photon-nucleon asymmetry A_1 are not suitable for the determination of PDFs because the structure function g_2 is not well known in QCD and the approximation

$$(A_1)^{theor} = g_1/F_1 - \gamma^2 g_2/F_1 \approx (g_1/F_1)^{theor} \quad (2)$$

used by some of the groups is *not* reasonable in the *preasymptotic* region because γ^2 cannot be neglected.

Bearing in mind the remarks above, let us discuss in more detail how to confront correctly the theoretical predictions to the available polarized inclusive DIS data:

i) First of all, one should include in the QCD fit of the world data *all* g_1/F_1 data available. These are the CLAS(p, d), JLab/Hall A(n), SLAC E143(p, d) and E155(p, d) data [1].¹

ii) For the rest of experiments: EMC(p), SMC(p, d) [2] and COMPASS(d) [3] at CERN, HERMES(p, d) [4] at DESY and E142(n), E154(n) at SLAC [5], only data on A_1 are presented. In the experiments at CERN and DESY only the asymmetry $A_{||}$ is measured. However, for different reasons the approximations $A_{||}/D \approx A_1 \approx g_1/F_1$ for CERN data and $A_{||}/[D(1 - \eta\gamma)] \approx A_1 \approx g_1/F_1$ for HERMES data are good ones. For the experiments at CERN, the γ^2 factor is very small and the term $\gamma^2 g_2/F_1$ can be neglected, while for the HERMES data the approximation $g_2 = 0$ is used and the effect of the non-zero value of g_2 is included in the systematic uncertainty of A_1 .² In the SLAC E142(n) and E154(n) experiments both $A_{||}$ and A_{\perp} have been measured and g_1/F_1 data could have been extracted, but the collaborations present only data on A_1 . Bearing in mind the kinematic region (E154) and the precision (E142) of these data, the approximation $A_1/(1 + \gamma^2) \approx g_1/F_1$ in Eq. (1) for them is reasonable.

To summarize, in the pure DIS region $A_1 \approx g_1/F_1$ and it does not matter which data are used in the QCD analysis. This is not the case when precise data in the preasymptotic region have to be used too. In that case one has to confront the QCD predictions to the data more carefully in order to extract the polarized PDFs correctly.

2.2 Methods of QCD analysis

In QCD, one can split g_1 and F_1 into leading (LT) and dynamical higher twist (HT) pieces

$$g_1 = (g_1)_{LT,TMC} + (g_1)_{HT}, \quad F_1 = (F_1)_{LT,TMC} + (F_1)_{HT}. \quad (3)$$

In the LT pieces in Eq. (3) the calculable target mass corrections (TMC) are included

$$g_1(x, Q^2)_{LT,TMC} = g_1(x, Q^2)_{LT} + g_1(x, Q^2)_{TMC}, \quad (4)$$

¹Note that excepting the E155 Collaboration, the other Collaborations present data on A_1 too. The corresponding values of A_1 and g_1/F_1 at the same (x, Q^2) are different, which means that the term $\gamma^2 g_2/F_1$ cannot be really neglected in the preasymptotic region and a fit to A_1 data instead of (g_1/F_1) , approximating $(A_1)^{theor}$ with $(g_1/F_1)^{theor}$ is *not* correct.

²Note that for the final inclusive HERMES A_1 data [6] the approximation $g_2 = 0$ is not used and the relation $A_1 \approx g_1/F_1$ does not hold.

$$F_1(x, Q^2)_{\text{LT,TMC}} = F_1(x, Q^2)_{\text{LT}} + F_1(x, Q^2)_{\text{TMC}}.$$

They are inverse powers of Q^2 kinematic corrections, which, however, effectively belong to the LT part of g_1 . Then, approximately

$$\frac{g_1}{F_1} \approx \frac{(g_1)_{\text{LT}}}{(F_1)_{\text{LT}}} \left[1 + \frac{(g_1)_{\text{TMC+HT}}}{(g_1)_{\text{LT}}} - \frac{(F_1)_{\text{TMC+HT}}}{(F_1)_{\text{LT}}} \right]. \quad (5)$$

Note that the LT pieces $(g_1)_{\text{LT}}$ and $(F_1)_{\text{LT}}$ are expressed in terms of the polarized and unpolarized PDFs, respectively. In what follows only the first terms in the TMC and HT expansions will be considered

$$\begin{aligned} g_1(x, Q^2)_{\text{TMC}} &= M^2/Q^2 g_1^{(1)}(x, Q^2)_{\text{TMC}} + \mathcal{O}(M^4/Q^4), \\ F_1(x, Q^2)_{\text{TMC}} &= M^2/Q^2 F_1^{(1)}(x, Q^2)_{\text{TMC}} + \mathcal{O}(M^4/Q^4); \end{aligned} \quad (6)$$

$$g_1(x, Q^2)_{\text{HT}} = h^{g_1}(x)/Q^2 + \mathcal{O}(\Lambda^4/Q^4), \quad 2xF_1(x, Q^2)_{\text{HT}} = h^{2xF_1}(x)/Q^2 + \mathcal{O}(\Lambda^4/Q^4). \quad (7)$$

The first terms of the HT pieces in Eq. (7) are shown in Fig. 1 and as seen, they are definitely different from zero and cannot be neglected in the preasymptotic region.

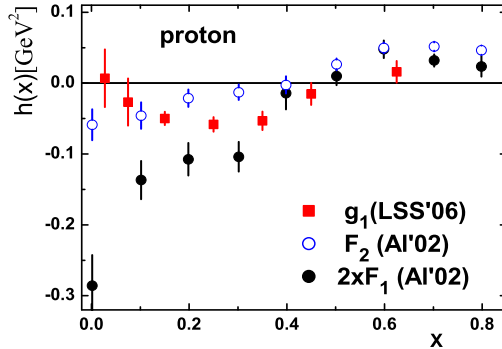


Figure 1. HT corrections to g_1 [10], F_2 and $2xF_1$ [11] structure functions.

There are essentially two methods to fit the data - taking or NOT taking into account the HT corrections to g_1 . According to the first [7], the data on g_1/F_1 have been fitted including the contribution of the first term $h(x)/Q^2$ in $(g_1)_{\text{HT}}$ and using the experimental data for the unpolarized structure function F_1

$$\left[\frac{g_1(x, Q^2)}{F_1(x, Q^2)} \right]_{\text{exp}} \Leftrightarrow \frac{g_1(x, Q^2)_{\text{LT,TMC}} + h^{g_1}(x)/Q^2}{F_1(x, Q^2)_{\text{exp}}} \quad (\text{Method I}). \quad (8)$$

According to the second approach [8] only the LT terms for g_1 and F_1 in (3) have been used in the fit to the g_1/F_1 data

$$\left[\frac{g_1(x, Q^2)}{F_1(x, Q^2)} \right]_{exp} \Leftrightarrow \frac{g_1(x, Q^2)_{LT}}{F_1(x, Q^2)_{LT}} \quad (\text{Method II}). \quad (9)$$

It is obvious that the two methods are equivalent in the pure DIS region where HT can be ignored. To be equivalent in the *preasymptotic* region requires a cancellation between the ratios $(g_1)_{\text{TMC+HT}}/(g_1)_{\text{LT}}$ and $(F_1)_{\text{TMC+HT}}/(F_1)_{\text{LT}}$ in (5). Then $(g_1)_{\text{LT}}$ obtained from the best fit to the data will coincide within the errors independently of the method which has been used. In Fig. 2 these ratios based on our results on target mass [9] and higher twist [10] corrections to g_1 , and the results on the unpolarized structure function F_1 are presented. Note that for the neutron target, $(g_1)_{\text{TMC+HT}}$ is compared with $(g_1)_{\text{LT}} \frac{(F_1)_{\text{TMC+HT}}}{(F_1)_{\text{LT}}}$ because of a node-type behaviour of $(g_1)_{\text{LT}}$. Also, LT means the NLO QCD approximation for both, g_1 and F_1 . As seen from Fig. 2, (TMC+HT) corrections to g_1 and F_1 in the ratio g_1/F_1 do not cancel and ignoring them using the second method is incorrect and will impact on the determination of the polarized PDFs.³

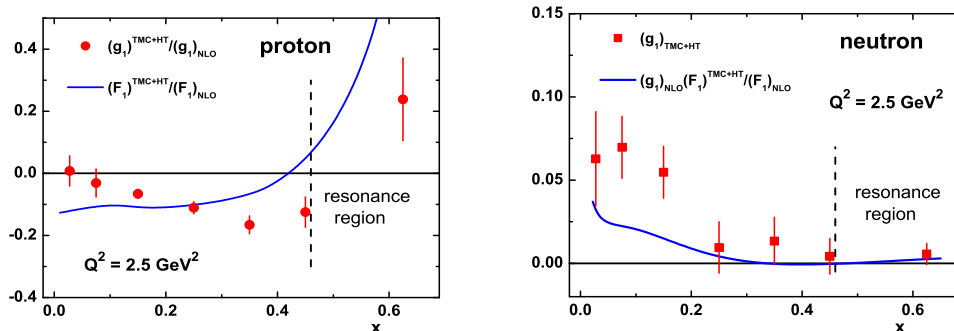


Figure 2. Comparison of the ratios of (TMC+HT)/LT for g_1 and F_1 structure functions for proton and neutron targets (see the text).

Modifications of the second method of analysis in which F_1 is treated in different way are also presented in the literature:

³Note that this result differs from our previous observation that the ratios $(g_1)_{\text{HT}}/(g_1)_{\text{LT}}$ and $(F_1)_{\text{HT}}/(F_1)_{\text{LT}}$ for a proton target approximately cancel for $x > 0.15$ at $Q^2 = 2.5 \text{ GeV}^2$ [12]. However, in a more precise analysis one should account for the TMC corrections in Eq. (5). Note that previously, for the calculation of the ratio $(F_1)_{\text{HT}}/(F_1)_{\text{LT}}$ the results of [11] were used, where a QCD analysis of the world unpolarized DIS data was performed using the cut $Q^2 \geq 2.5 \text{ GeV}^2$. This cut excludes a lot of data in the preasymptotic region which influence the determination of the HT corrections to F_1 . Fig. 2 is based on a new analysis of the ratio $(F_1)_{\text{TMC+HT}}/(F_1)_{\text{LT}}$ [13].

i) Blumlein, Bottcher [14] and COMPASS [3], where instead of $(F_1)_{LT}$ in (9), $(F_1)_{exp}$ has been used in the fit to the data

$$\left[\frac{g_1(x, Q^2)}{F_1(x, Q^2)} \right]_{exp} \Leftrightarrow \frac{g_1(x, Q^2)_{LT}}{F_1(x, Q^2)_{exp}} ; \quad (10)$$

ii) AAC Collaboration [15], where F_1 is expressed in terms of F_2 and R , and for them: $(F_2)_{LT}$ and R_{exp} have been used, respectively

$$A_1(x, Q^2)_{exp} \approx \left[\frac{g_1(x, Q^2)}{F_1(x, Q^2)} \right]_{exp} \Leftrightarrow \frac{g_1(x, Q^2)_{LT}}{F_2(x, Q^2)_{LT}} 2x(1 + R(x, Q^2)_{exp}) . \quad (11)$$

As mentioned above, the approximation for A_1 in (11) is not correct for most of the data sets used in the fit.

Note that when the second method or its modifications are used, the HT effects of g_1 are apparently absorbed into the extracted PDFs, which thus differ from those determined in the presence of HT (for more details see the discussion below), but, of course, not all the data can be fitted satisfactorily. On other hand, the extracted PDFs in the framework of the second method and corresponding to fits (9 - 11) should all be different due to the HT corrections to F_1 (see Fig. 1) which are included in Eq. (10) but not in Eq. (9), and only partly in Eq. (11). So, using the different denominators in (9 - 11) one will obtain different values for the free parameters associated with the input polarized PDFs after fitting the data.

3 Polarized Parton Densities

We will discuss in this section in more detail how the results on polarized PDFs depend on the method used for their determination. To illustrate this dependence we will compare the NLO LSS'06 set of polarized parton densities [10] determined by Method I with those obtained by COMPASS [3], DSSV [16] and AAC Collaboration [17] using Method II or its modifications.

3.1 Comparison between LSS'06 and COMPASS PDFs

To obtain the LSS'06 PDFs we used Method I (Eq. 8) in the QCD analysis of the the world data on polarized inclusive DIS ([1]-[5]), i.e. the HT corrections to g_1 were taken into account. For the LT term we have used the NLO QCD approximation in the \overline{MS} renormalization scheme. In their analysis COMPASS has used Eq. (10), but the CLAS data

from [1] were not included in their fit.⁴ In both the analyses the experimental data for the unpolarized structure function F_1 were used. Thus what is fitted by $(g_1^N)_{LT}(\text{COMPASS})$ is significantly different from what is fitted by our $(g_1^N)_{LT}(\text{LSS})$, i.e.

$$g_1^N(x, Q^2)_{LT}(\text{COMPASS}) = g_1^N(x, Q^2)_{LT, \text{TMC}}(\text{LSS}) + h^N(x)/Q^2 \equiv (g_1^N)_{\text{tot}}^{\text{LSS}} \quad (N = p, n, d). \quad (12)$$

Note that for $(g_1)_{LT}$ COMPASS has also used the NLO QCD approximation in the $\overline{\text{MS}}$ scheme. As a result, $(g_1)_{\text{tot}}^{\text{LSS}}$ and $(g_1)_{LT}(\text{COMPASS})$ obtained from the fit are almost identical, but the LT terms of g_1 corresponding to LSS and COMPASS fits are different for $x < 0.1$ where the HT corrections to g_1^d cannot be neglected. This fact is illustrated in Fig. 3 for g_1^d where the COMPASS data are also presented. We have found that the

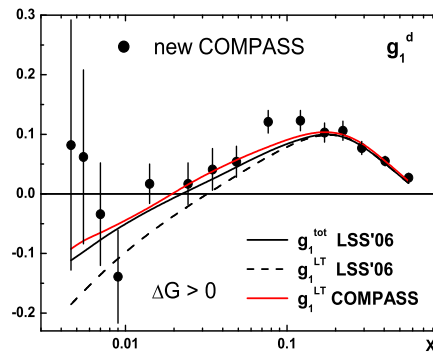


Figure 3. Comparison between $(g_1)_{\text{tot}}(\text{LSS})$ and $(g_1)_{LT}(\text{COMPASS})$ obtained from the fit with the COMPASS data at measured x and Q^2 . Error bars represent the total (statistical and systematic) errors. The $(g_1)_{LT}(\text{LSS})$ curve is also shown.

HT contribution to $(g_1^d)_{\text{tot}}$, $h^d(x)/Q^2$, is positive and large, up to 40% of the magnitude of $(g_1^d)_{LT}$ in the small x region, where Q^2 is small ($Q^2 \sim 1 - 3 \text{ GeV}^2$). As a consequence, the HT effects are effectively absorbed in the COMPASS PDFs. A crucial point is that the COMPASS analysis does not include CLAS data, which are entirely in the pre-asymptotic region, and for which the HT effects are essential. In Fig. 4 the COMPASS PDFs corresponding to a positive solution for ΔG are compared with those obtained by LSS'06. As seen from Fig. 4, except for $(\Delta u + \Delta \bar{u})$ the other PDFs differ, especially those of the strange quarks and gluons.

⁴Using this method one cannot achieve an acceptable value of χ^2 for the CLAS data which are entirely in the preasymptotic region [18].

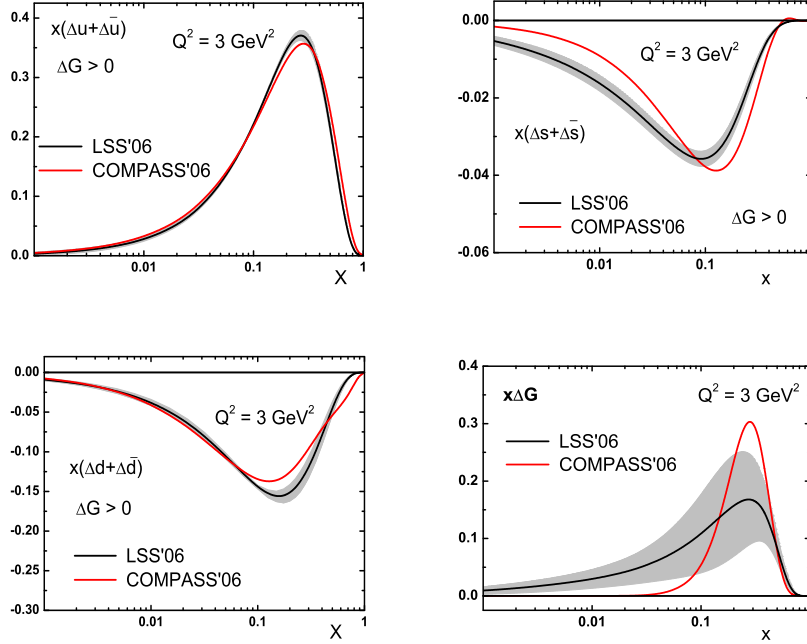


Figure 4. Comparison between NLO($\overline{\text{MS}}$) LSS'06 polarized PDFs and those obtained by COMPASS.

3.2 Comparison between LSS'06 and DSSV PDFs

Recently the DSSV group has presented results on NLO($\overline{\text{MS}}$) polarized PDFs [16] obtained from the first global analysis of polarized DIS, SIDIS and RHIC polarized pp scattering data. Due to the SIDIS data a flavor decomposition of the polarized sea is achieved. For the fit to the inclusive DIS data the second method (9) was used, i.e., a NLO QCD approximation for $(g_1)_{\text{LT}}$ and $(F_1)_{\text{LT}}$ in the ratio g_1/F_1 . The unpolarized structure function $F_1(x, Q^2)_{\text{LT}}$ was calculated using the NLO MRST'02 parton densities [19]. The difference between $F_1(x, Q^2)_{\text{NLO}}$ and the phenomenological parametrization of the data, $F_1(x, Q^2)_{\text{exp}}$, used in our analysis [10] is illustrated in Fig. 5. It is a measure of the size of the TM and HT corrections $F_1(x, Q^2)_{\text{TMC+HT}}$ to F_1 which cannot be ignored in the pre-asymptotic region. Note that in the MRST fit to the unpolarized data the preasymptotic region was excluded precisely in order to eliminate the TM and HT corrections. That is why $F_1(\text{MRST})_{\text{NLO}}$ differ from $(F_1)_{\text{exp}}$ in the preasymptotic region where the TM and HT corrections to F_1 cannot be ignored.

It is important to mention also that in the preasymptotic region for large x and lower Q^2 ($x > 0.40$, 0.47 for JLab and SLAC/E143 data, respectively), the kinematic factor $\gamma^2 = 4M^2x^2/Q^2$ is larger than $R(x, Q^2)$. Then it follows from the relation between F_1

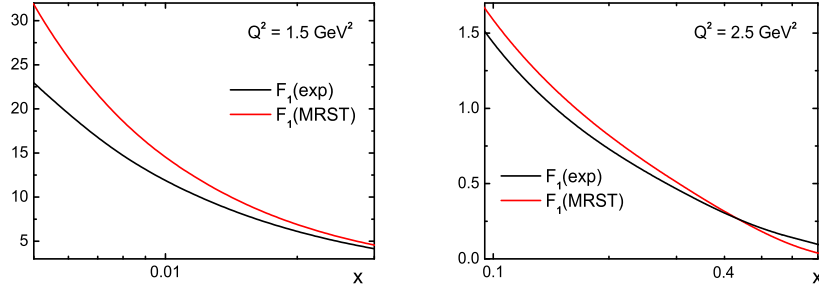


Figure 5. Comparison between $F_1^p(\text{MRST})_{\text{NLO}}$ and $(F_1^p)_{\text{exp}}$ unpolarized structure functions at $Q^2 = 1.5 \text{ GeV}^2$ (left) and $Q^2 = 2.5 \text{ GeV}^2$ (right).

and F_2

$$2xF_1(x, Q^2) = F_2(x, Q^2) \frac{1 + \gamma^2}{1 + R(x, Q^2)} \quad (13)$$

that in this region $2xF_1 > F_2$ and, as a consequence,

$$F_L(x, Q^2) = F_2(x, Q^2) - 2xF_1(x, Q^2) \quad (14)$$

is negative, in contrast to what follows from pQCD, i.e. that $(F_L)_{\text{LT}}$ should be always positive. So, F_L could become negative in the preasymptotic region due to HT corrections. We consider it is important to test this observation by fitting the data on unpolarized structure functions F_2 and F_L which will become available at JLab in the near future.

The main features of the results of the fits obtained by LSS (Method I) and DSSV (Method II) are illustrated in Fig. 6 for a proton target. As expected, the curves corresponding to the ratios $g_1^{\text{tot}}(\text{LSS})/(F_1)_{\text{exp}}$ and $g_1(\text{DSSV})_{\text{NLO}}/F_1(\text{MRST})_{\text{NLO}}$ practically coincide although different expressions were used for g_1 and F_1 in the fit (see the left panel of Fig. 6; the difference between them for $x > 0.2$ will be discussed later). In the right panel of Fig. 6 the LSS and DSSV LT(NLO) pieces of g_1 are compared for a proton target. Surprisingly they coincide for $x > 0.1$ although the HT corrections, taken into account in LSS'06 and ignored in the DSSV analysis, do NOT cancel in the ratio g_1/F_1 in this region, as has already been discussed above. The understanding of this puzzle is connected with the fact that in the DSSV fit to all available g_1/F_1 data a factor $(1 + \gamma^2)$ was introduced on the RHS of Eq. (9)

$$\left[\frac{g_1(x, Q^2)}{F_1(x, Q^2)} \right]_{\text{exp}} \Leftrightarrow \frac{g_1(x, Q^2)_{\text{LT}}}{(1 + \gamma^2)F_1(x, Q^2)_{\text{LT}}} \quad (15)$$

(Note that for the fit to the A_1 data Eq. (9) was used.)

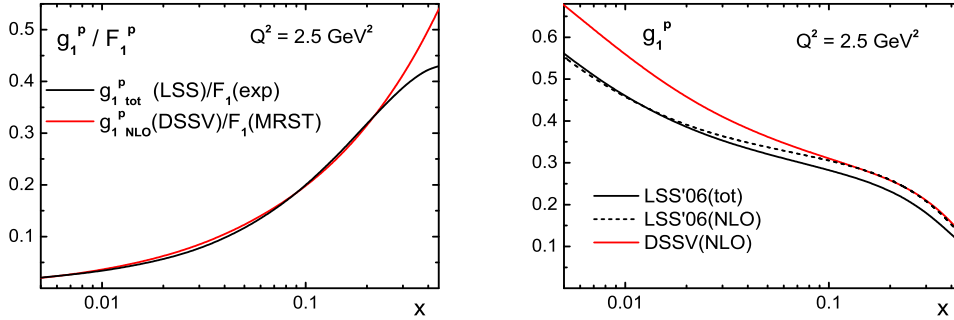


Figure 6. Comparison between: the ratios $g_1^{tot}(\text{LSS})/(F_1)_{\text{exp}}$ and $g_1(\text{DSSV})_{\text{NLO}}/F_1(\text{MRST})_{\text{NLO}}$ (**left**); $g_1(\text{LSS})_{\text{NLO}}$ and $g_1(\text{DSSV})_{\text{NLO}}$ (**right**). The LSS results correspond to the node-type solution for $x\Delta G(x, Q^2)$.

There is no rational explanation for such a correction. The authors point out [20] that it is impossible to achieve a good description of the g_1/F_1 data, especially of the CLAS ones, without this correction (see Fig. 7). As seen from Fig. 7, the theoretical curves lie systematically above the data which are badly fitted without introducing the $(1 + \gamma^2)$ factor.

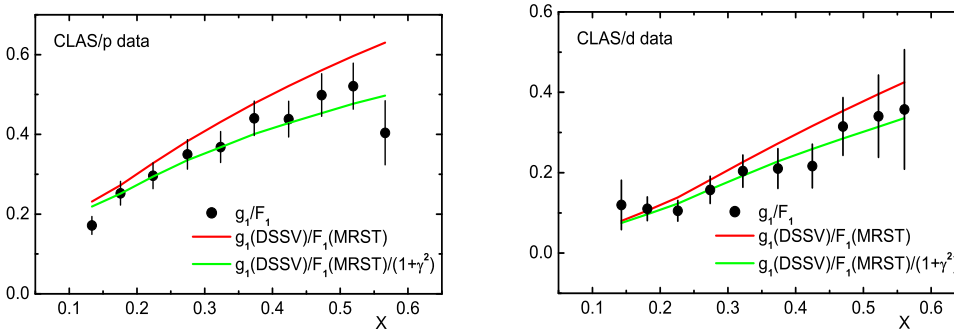


Figure 7. CLAS g_1/F_1 data compared to the theoretical DSSV curves accounted or not for the $(1 + \gamma^2)$ factor.

It turns out empirically that the $1/(1 + \gamma^2)$ factor accidentally more or less accounts for the TM and HT corrections to g_1 and F_1 in the ratio g_1/F_1 . The relation

$$1 + \frac{(g_1)_{\text{TMC+HT}}}{(g_1)_{\text{LT}}} - \frac{(F_1)_{\text{TMC+HT}}}{(F_1)_{\text{LT}}} \approx \frac{1}{(1 + \gamma^2)} \quad (16)$$

is satisfied with an accuracy between 4% and 18% for the CLAS proton data ($x > 0.1$ and Q^2 between 1 and 4 GeV^2). That is the reason why the LT(NLO) pieces of g_1^p obtained by LSS and DSSV are in a good agreement for $x > 0.1$ (see the right panel of fig. 6). Also, why the curve in Fig 6 (left) corresponding to $g_1(\text{DSSV})_{\text{NLO}}/F_1(\text{MRST})_{\text{NLO}}$ lies above the one of $g_1^{\text{tot}}(\text{LSS})/(F_1)_{\text{exp}}$. Including the $(1+\gamma^2)$ factor in (15) would make the curves almost identical. It is important to mention that introducing the $(1 + \gamma^2)$ factor does not help at $x < 0.2$ because it is small in this region and cannot mimic the difference between TM and HT corrections to g_1 and F_1 (LHS of Eq. (16)) for proton as well as for neutron target (see Fig. 2). That is why the LT(NLO) pieces of g_1^p obtained by LSS and DSSV groups differ in this region - the smaller x is, the greater is the difference (see Fig. 6 (right)). To summarize: It is impossible to describe the precise data in the preasymptotic region like the CLAS data using the second method. Its empirical modification by introducing the $(1 + \gamma^2)$ factor accounts approximately for the TM and HT effects, but only in the x region: $x > 0.1, 0.2$ for proton and neutron targets, respectively.

The NLO($\overline{\text{MS}}$) PDFs determined from LSS'06 and DSSV analyses are compared in Fig. 8. The AAC'08 PDFs [17] obtained from a combined NLO QCD analysis of inclusive DIS and RHIC π^0 -production data are also presented. Note that for the fit to DIS data

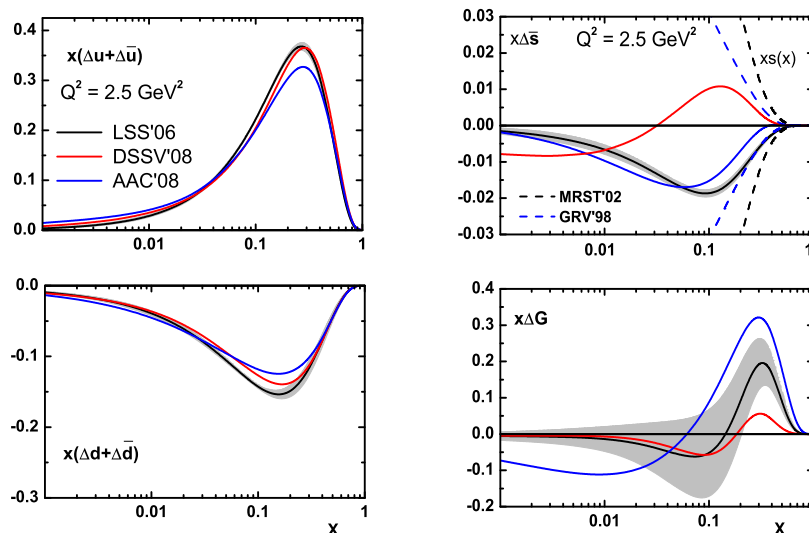


Figure 8. Comparison between LSS'06, DSSV and AAC'08 NLO PDFs in ($\overline{\text{MS}}$) scheme.

AAC have used the modification (11) of the second method and that the RHIC data impact mainly on ΔG . Note also that all these analyses include the precise CLAS data in the preasymptotic region. The results are presented for the sums $(\Delta u + \Delta \bar{u})$ and $(\Delta d + \Delta \bar{d})$

because they can only be separated using SIDIS data (the DSSV analysis). Although the first moments obtained for the PDFs are almost identical, the polarized quark densities themselves are different, especially $\Delta\bar{s}(x)$ (in all the analyses $\Delta s(x) = \Delta\bar{s}(x)$ is assumed).

Let us discuss the impact of HT effects on $(\Delta u + \Delta\bar{u})$ and $(\Delta d + \Delta\bar{d})$ parton densities which should be well determined from the inclusive DIS data. $(\Delta u + \Delta\bar{u})$ extracted by LSS and DSSV are well consistent. As was discussed above the HT effects for the proton target are effectively accounted for in the DSSV analysis for $x > 0.1$ by the introduction of the $(1 + \gamma^2)$ factor. However, this factor cannot account for the HT effects for a neutron target at $x < 0.2$ (see Fig. 2) and the impact of higher twist on $(\Delta d + \Delta\bar{d})$ determined by DSSV is demonstrated in Fig. 8. The positive HT effects are absorbed into $(\Delta d + \Delta\bar{d})_{\text{DSSV}}$ and it is thus less negative in this region. The influence of HT effects at small x (not accounted for by the DSSV group) on both parton densities is not sizable because of two reasons: first, their values are small and second, the data in this region are not precise enough to indicate the impact of higher twist on their values. The impact of HT effects on both $(\Delta u + \Delta\bar{u})_{\text{AAC}}$ and $(\Delta d + \Delta\bar{d})_{\text{AAC}}$ is larger because the AAC Collaboration has not taken them into account at all, and in addition, the incorrect approximation $A_1 \approx g_1/F_1$ for some of the data in the preasymptotic region has been used. The difference between the strange sea densities $\Delta\bar{s}(x, Q^2)_{\text{LSS}}$ and $\Delta\bar{s}(x, Q^2)_{\text{AAC}}$ for $x > 0.1$ is due to the different positivity conditions which have been used by the two groups. Note also that the positivity condition $|\Delta G(x, Q^2)| \leq G(x, Q^2)$ is not satisfied for the polarized gluon density obtained by AAC, which suggests it is not physical.

In contrast to a negative $\Delta\bar{s}(x, Q^2)$ obtained in all analyses of inclusive DIS data, the DSSV global analysis yields a changing in sign $\Delta\bar{s}(x, Q^2)$: positive for $x > 0.03$ and negative for small x . Its first moment is negative (practically fixed by the SU(3) symmetric value of a_8) and almost identical with that obtained in the inclusive DIS analyses. It was shown [21] that the determination of $\Delta\bar{s}(x)$ from SIDIS strongly depends on the fragmentation functions (FFs) and the new FFs [22] are crucially responsible for the unexpected behavior of $\Delta\bar{s}(x)$. So, obtaining a final and unequivocal result for $\Delta\bar{s}(x)$ remains a challenge for further research on the internal spin structure of the nucleon.

4 Summary

The fact that more than a half of the present polarized DIS data are in the preasymptotic region makes the QCD analysis of the data more complex and difficult. In contrast to the unpolarized case, the $1/Q^2$ terms (*kinematic* - γ^2 factor, target mass corrections, and *dynamic* - higher twist corrections to the spin structure function g_1) cannot be ignored,

and their role in determining the polarized PDFs is important. Sets of polarized PDFs extracted from the data using different methods of QCD analysis, accounting or not accounting for the kinematic and dynamic $1/Q^2$ corrections, are considered. The impact of higher twist effects on the determination of the parton densities is demonstrated. It is pointed out that the very accurate DIS data in the preasymptotic region require a more careful matching of QCD to the data in order to extract the polarized PDFs correctly.

Acknowledgments

This research was supported by the JINR-Bulgaria Collaborative Grant, by the RFBR Grants (No 08-01-00686, 09-02-01149) and by the Bulgarian National Science Foundation under Contract 288/2008. One of the authors (D.S) is grateful to Theory Division at CERN for providing the facilities essential for the completion of this work.

References

- [1] K.V. Dharmawardane *et al.* (CLAS Collaboration), Phys. Lett. B **641**, 11 (2006); X. Zheng *et al.* (JLab/Hall A Collaboration), Phys. Rev. Lett. **92**, 012004 (2004); K. Abe *et al.* (SLAC E143 Collaboration), Phys. Rev. D **58**, 112003 (1998); P.L. Anthony *et al.* (SLAC E155 Collaboration), Phys. Lett. B **463**, 339 (1999); **493**, 19 (2000).
- [2] J. Ashman *et al.* (EMC Collaboration), Phys. Lett. B **206**, 364 (1988); Nucl. Phys. **B328**, 1 (1989); B. Adeva *et al.* (SMC Collaboration) Phys. Rev. D **58**, 112001 (1998).
- [3] V.Y. Alexakhin *et al.* (COMPASS Collaboration), Phys. Lett. B **647**, 8 (2007).
- [4] A. Airapetian *et al.* (HERMES Collaboration), Phys. Rev. **D71**, 012003 (2005).
- [5] P.L. Anthony *et al.* (SLAC E142 Collaboration), Phys. Rev. **D54**, 6620 (1996); K. Abe *et al.* (SLAC/E154 Collaboration), Phys. Rev. Lett. **79**, 26 (1997).
- [6] A. Airapetian *et al.* (HERMES Collaboration), Phys. Rev. **D75**, 012007 (2007).
- [7] E. Leader, A.V. Sidorov, and D.B. Stamenov, Phys. Rev. D **67**, 074017 (2003).
- [8] M. Glück, E. Reya, M. Stratmann, and W. Vogelsang, Phys. Rev. D **63**, 094005 (2001).
- [9] A.V. Sidorov and D.B. Stamenov, Mod. Phys. Lett. **A21**, 1991 (2006).

- [10] E. Leader, A.V. Sidorov, and D.B. Stamenov, Phys. Rev. D **75**, 074027 (2007).
- [11] S.I. Alekhin, Phys. Rev. D **68**, 014002 (2003).
- [12] E. Leader, A.V. Sidorov, and D.B. Stamenov, in the Proceedings of 16th International Workshop on Deep Inelastic Scattering and Related Subjects (DIS2008), 7-11 April, 2008, London, UK (edited by R. Devenish and J. Ferrando, Science Wise Publishing, 2008, 206 (arXiv:0806.2094 [hep-ph])).
- [13] D.B. Stamenov, unpublished.
- [14] J. Blumlein, H. Bottcher, Nucl. Phys. **B 636**, 225 (2002).
- [15] AAC, M. Hirai et al., Phys. Rev. **D 69**, 054021 (2004).
- [16] D. de Florian, R. Sassot, M. Stratmann, and W. Vogelsang, Phys. Rev. Lett. **101**, 072001 (2008); arXiv:0904.3821 [hep-ph].
- [17] M. Hirai and S. Kumano, arXiv:0808.0413 [hep-ph].
- [18] R. Winmolders, private communication.
- [19] A.D. Martin, R.G. Roberts, W.J. Stirling, and R.S. Thorne, Eur. Phys. J. C **28**, 455 (2003).
- [20] R. Sassot, private communication.
- [21] M. Alekseev et. al. (COMPASS Colaboration), arXiv:0905.2828 [hep-ex].
- [22] D. de Florian, R. Sassot, and M. Stratmann, Phys. Rev. D **75**, 114010 (2007); D **76**, 074033 (2007).